 doi:10.20944/preprints202105.0085.v1

Article

Effect of Li concentration on the structural and optical properties of $Co_{1-x}Li_xCr_2O_4$ chromate nanoparticles prepared by sol-gel method

Muhammad Saeed[1], Malika Rani[2], Kiran Batool[2], Hafiza Batool[2], Aisha younus[3], Sikander Azam[4*], Arshad Mehmood[5], Bakhtiarul Haq[6], Thamraa Alshahrani[7*], Muhammad Maqbool[8*]

1. East China University of Technology, Nanchang, 330013, China.
2. Department of Physics, The Women University Multan, Pakistan.
3. Department of Physics, University of Agriculture Faisalabad, Pakistan.
4. Faculty of Engineering and Applied Sciences, Department of Physics, RIPHAH International University I-14 Campus Islamabad, Pakistan.
5. National Institute of Laser& Optronics, Nilore, Islamabad, Pakistan.
6. AFMOL, King Khalid University, Saudi Arabia.
7. Department of Physics, College of Science, Princess Norah Bint Abdulrahman University, Riyadh, Saudi Arabia.
8. Department of Clinical & Diagnostic Sciences, Health Physics Program, the University of Alabama at Birmingham, Birmingham, AL 35294, USA.

* Corresponding-Authors: Muhammad Maqbool: mmaqbool@uab.edu
Sikander Azam: Sikander.physicst@gmail.com,
Thamraa Alshahrani: thmalshahrani@pnu.edu.sa

Abstract: $CoCr_2O_4$ and doped lithium $Co_{1-x}Li_xCr_2O_4$ chromate powder and nanoparticles were prepared by modified by sol-gel method. The morphological and structural properties of nano chromates were investigated by x-ray diffraction (XRD), scanning electron microscopy (SEM), Raman spectroscopy and Photoluminescence (PL). Nanoparticles of doped lithium were synthesized by adding appropriate amount of cobalt nitrate, chromium nitrate, lithium nitrate and 1,2 Ethanediol as a complexing agent. The sample were heated at 105 ˚C for ten hours in oven to obtain dry gel. Calcination temperature for these samples was 700˚C for 3 hours in a furnace. The particle size of parent compound ranges from 4.4 nm to 11 nm, determined by SEM. The tendency of particles to form the aggregates with the increased annealing temperature was observed. The SEM and optical characterization of this compound has shown the sol gel derived material may be successfully used as an effective doped lithium cobalt ceramic pigment with controlled variation in structural and optical properties. SEM images showed that spherical like doped particle have diameter 33nm. From PL spectra Nano structure shows band gap 2.5ev and when we doped Lithium in it band gap decreases and become 1.19ev, which is associated to band gap transition.

Keywords: Sol gel process, Pigments, Cobalt Chromate, Nanoparticles, Synthesis, Lithium,

1. Introduction

A tiny particle as small as 1 to 100 nanometers in size is called a nanoparticle. Due to its very low size a human eye cannot see or detect a nanoparticle. The unique aspect of nanoparticles is that they can exhibit significantly different physical and chemical properties to their bulk material counterparts [1,2].

Metallic and non-metal nanoparticles have been gaining attraction due to their unique applications in environmental, biomedical, optical and electronic industries [3,4]. Metal oxides nanoparticles are among the widest used manufactured nanomaterials because of their unique properties [5]. The properties that make the nanophase structures indispensable tools in modern nanotechnology are their various nonlinear optical properties, higher ductility at elevated temperatures than the coarse-grained ceramics, cold welding properties, superparamagnetic behaviour,

Preprints (www.preprints.org) | NOT PEER-REVIEWED | Posted: 6 May 2021 doi:10.20944/preprints202105.0085.v1

unique catalytic, sensitivity, and selective activity. For example, the melting point of the nanosized material is lower than that of a bulk material with the same composition [6]. At the same time, nanoparticles exhibit unusual adsorptive properties and fast diffusivities and they are not stable in critical conditions [7].

Cobalt chromite nanoparticles are usually synthesized at various temperatures by hydrothermal treatment of chromium and cobalt nitrates in a mixture of water and ethylene glycol. $CoCr_2O_4$ nanoparticles have different properties like high temperature, high resistance to light and chemicals they are widely used in industrial and commercial scale [8,9].

Nanoparticles Metal oxides and their mixtures have been used as ceramic pigments. Pigments have been in demand for several applications like chemical and thermal stability, hiding and tinting power, particle size. Mixed metal oxides with general spinel formula AB_2O_4 are characteristics for high thermal and chemical stability and for mechanical resistance [10,11]. Spinel structure has two types, one is known as normal spinel, which is characterized by A^{+2} cations occupying tetrahedral position and the other characterized by cations B^{+3} occupying octahedral structure. The subordinate possible structure is inverse spinel, that is also characterized by A^{+2} occupying one half of the tetrahedral site and B^{+3} another half of the octahedral position and all tetrahedral coordination positions [12]. Inverse spinel structure can be affected by temperature and pressure during its synthesize [13].

$CoCr_2O_4$ are normal ferromagnetic spinel with ions Co^{+2} occupying the tetrahedral A sites and the octahedral B sites occupied by Cr^{+3} ions [14]. The compound system undergoes a long-term order of ferromagnetism below ferromagnetic curie temperature of Tc=94 K [15]. Magnetic tangled phase diagram is obtained by the interaction of Co^{+2} and Cr^{+3} [16]. Under the spiral ordering at Ts=26K temperature the system is multiferroic [17]. The phase transition present occurs at the Lock-in transition temperature Tl=15K [18]. Nanoparticles of $CoCr_2O_4$ possess magnetic properties [14-16]. Strong cluster glass like performance have been described for nanoparticles size of 3.1 nm [19]. Since above 310 K, $CoLiCr_2O_4$ crystallizes and attains cubic normal spinel structure, therefore, the crystal structure becomes tetragonal due to Jahn-Teller manipulation in that temperature range [20]. Lowering temperature below 65 K, the crystal structure farther transforms into orthorhombic phase [21]. A deformation within the same orthorhombic phase has been distinguished at T=30 K [13]. The magnetic properties of $CoCr_2O_4$ and $CoLiCr_2O_4$ are different so for Ni doped $CoCr_2O_4$, co-precipitation method used to synthesize particles which contain standard size 80-100 nm, are delineated [22]. The property of magnetization of applied magnetic field displays a thin characteristic measured for $Co_{0.5}Ni_{0.5}Cr_2O_4$ nanoparticles developed through sol-gel process at T=10 K, which is missing in $CoLiCr_2O_4$ and $CoCr_2O_4$ [23].

In our present work, we have synthesized cobalt doped lithium chromates nanoparticles by sol gel method, which is easy to use, and environment friendly. Sol gel method requires low temperature and shorter calcination to obtain the desired product [24]. Comparison between two compounds base and doped cobalt chromates with different transition metal concentration with a step of 0.2 is made. The phase composition crystalize size and new spinel composition were investigated in this study.

2. Materials and Methods

To synthesize and fabricate $CoCr_2O_4$, and Li doped in cobalt chromate for the formation of lithium chromate we used lithium nitrate, cobalt nitrate, and chromium nitrate solution. 100 ml distilled water and 1,2 Ethendiol (as a complexing agent) was added to solution. In this process 100ml purified water was taken in a beaker and excess amount of lithium nitrates, cobalt and chromium were added. The beaker was then heated and constantly stirred at a temperature of 60-65 ^{0}C. The heating continued for an hour until the solution became homogenous then 1,2 ehanediol (as a complexing agent) was added to the reaction solution to form gel. Intensive green gel was obtained after heating it for about 4 hours. This process is shown in Figure 1. The gel was dried in a DHG-9202 Oven at 105 ^{0}C for ten hours. As a result, green colored powder was obtained. A grinder and agate motor were used

Preprints (www.preprints.org) | NOT PEER-REVIEWED | Posted: 6 May 2021 doi:10.20944/preprints202105.0085.v1

to grind the powder well. VULCAN-D550 furnace was used to sinter the powder of $CoCr_2O_4$ and $Co_{1-x}Li_xCr_2O_4$ at 700^{0}C for 3 hours to obtain greenish color nanoparticles. At the end, the powder, which is obtained, greenish in color. This synthesis and fabrication process is shown in figure 1. The nanoparticles were characterized for their structural and optical properties using XRD, SEM, Raman spectroscopy and PL.

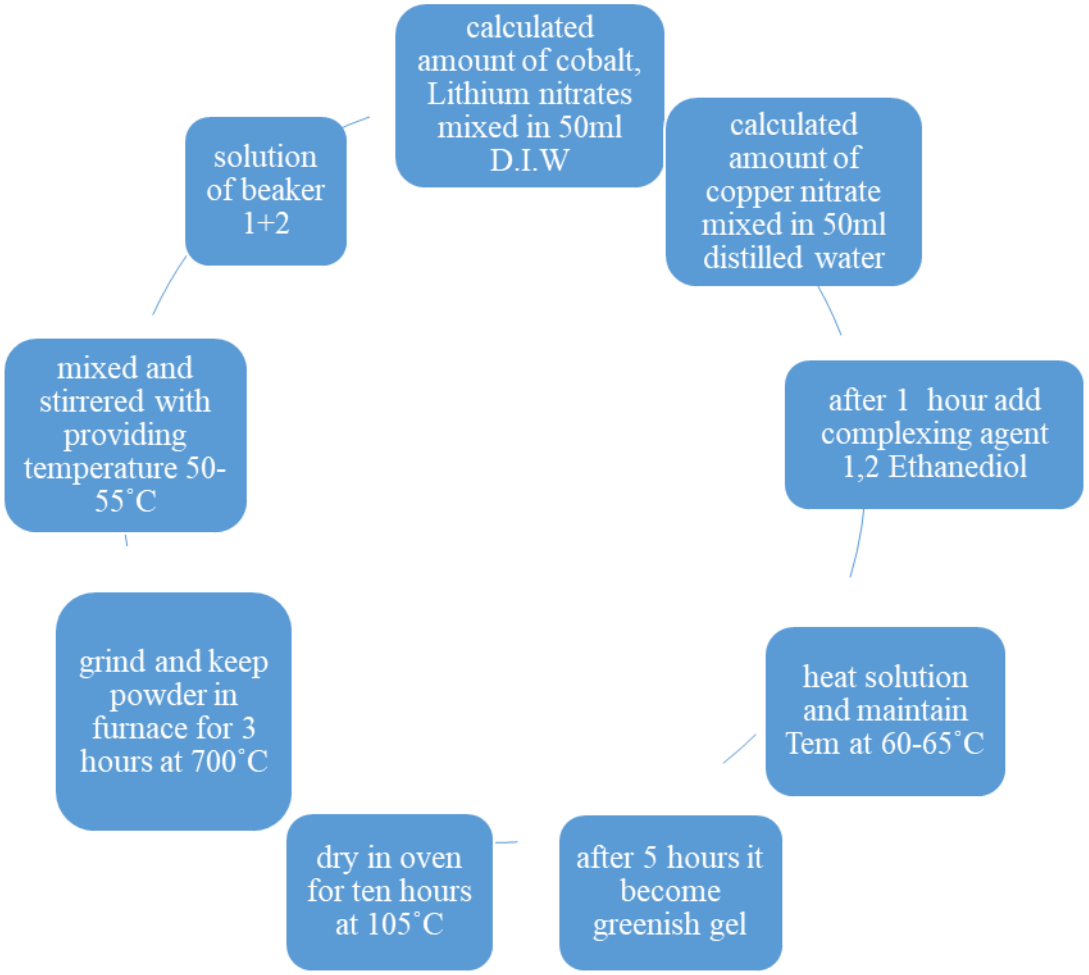

Figure 1. Schematic flowchart of manufacturing$CoCr_2O_4$, $CoLiCr_2O_4$ nanoparticle

3. Results and Discussion

3.1.1. XRD Analysis.

Information of phase and crystal structure of cobalt chromite is obtained through X-ray diffraction technique. The range of angle 2Θ of XRD pattern ranges from 15^0 to 60^0. XRD pattern of cobalt chromite is shown in Figure 2. Single phase of cobalt chromite is obtained at calcination temperature of 700 ^{0}C. XRD peaks, corresponding to 700^{0}C, were obtained at 15.5^0, 30.5^0, 35.5^0, 40.5^0, 45^0, 50^0 and 55.5^0. A high pure cubic single-phase structure of cobalt chromite is synthesized through this process. Single 124 phase of cobalt chromite is obtained with reference code COD REV218120 2019.09 at 700^{0}C temperature. XRD analysis of cobalt chromite shows that the lattice parameter a and c range from 8.328-8.412 Å. Wavelength 1.541874 Å of cobalt chromite is obtained from XRD peaks.

X-ray diffraction pattern of Ni powders substituted $Co_{1-x}Li_xCr_2O_4$ depending on calcination temperature was attained by sol gel process. Phase composition analysis shows that sample with higher substitution rate with x= 0.2, 0.4 and 0.6 have no single phase for all temperatures. X-ray diffraction explains the substitution of cobalt from nickel chromite in proceeds by steady transformation of cubic $CoCr_2O_4$ crystalline phase into cubic $CoLiCr_2O_4$ spinel state. The fact that majority powders are not in single phase is not critical, since the main goal of pigmentary field is to achieve the proper parameters of the pigments for application in industry [25].

Preprints (www.preprints.org) | NOT PEER-REVIEWED | Posted: 6 May 2021 doi:10.20944/preprints202105.0085.v1

The estimated size of crystallite size of cobalt chromites is 48.9nm obtained from heat treatment 700°C. For the powders, $Co_{1-x}Li_xCr_2O_4$ crystallite size varied after heat treatment 700°C 33.2to 44.4nm. The crystallite size increases less than 10nm for all temperature in range.

The average particle size can be calculated using Bragg's equation, $n\lambda = 2dSin\Theta$, where **n** is an integer, **Θ** is the angle between incident and scattered ray, **d** is the inter-spacing distance and **λ** is the wavelength associated with the particle. Crystal size **D** of a particle can also be calculated by using Scherrer's equation, $D = K\lambda/\beta Cos\Theta$, where **K** is crystalline shape constant.

XRD results show that the powder form nanoparticles achieved from sol gel process are more homogenous than obtained by other technique. However, phase composition is identical to parent compound, yet, morphology of synthesized pigments differed significantly.

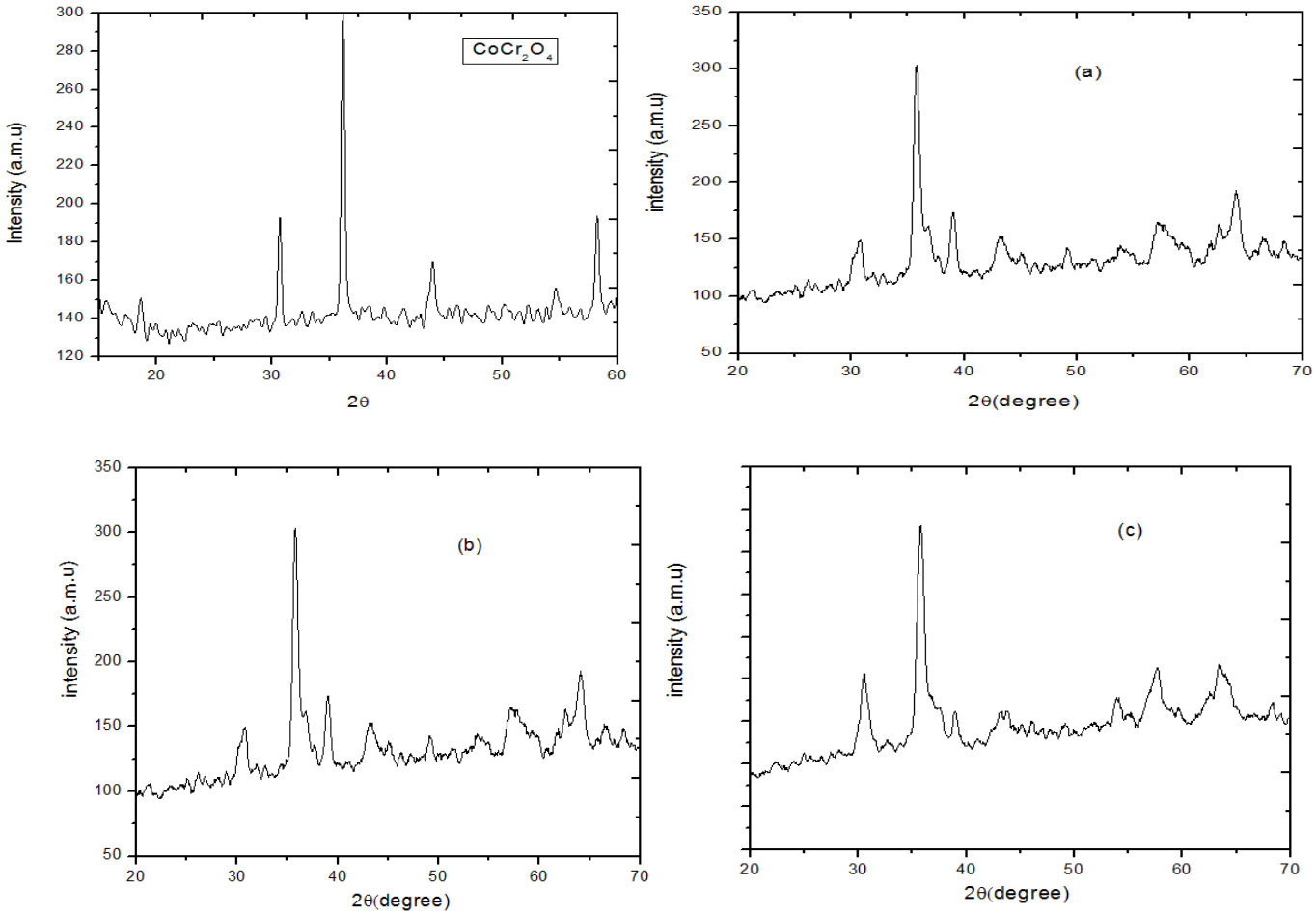

Figure 2. XRD analysis of $Co_{1-x}Li_xCr_2O_4$ (a) x=0.2, (b) x=0.4 (c) x=0.6

3.2. SEM Analysis.

Morphology of samples obtained by methods of synthesis is quite different than others. SEM micrograph of sol gel obtained samples of $CoLiCr_2O_4$ heated at 700°C and $CoCr_2O_4$ have different morphological features as shown in Figure 3. Very small spherical nanosized particles of $CoCr_2O_4$ synthesized showing high degree of agglomeration.

Different shaped and bigger sized (150-200 nm) particles of $CoLiCr_2O_4$ were obtained in synthesis. Surface morphology of doped cobalt chromite is very similar to cobalt chromite. The obtain powder largely consist of irregular, sub-micron shape particles of size 110 nm – 0.5 μm, which resulted in a few large agglomerates with porous microstructure.

Preprints (www.preprints.org) | NOT PEER-REVIEWED | Posted: 6 May 2021 doi:10.20944/preprints202105.0085.v1

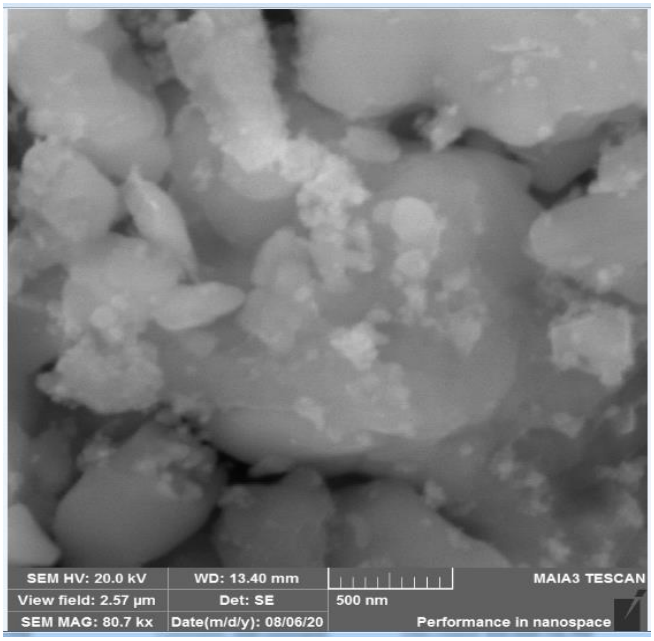

x = 0.0

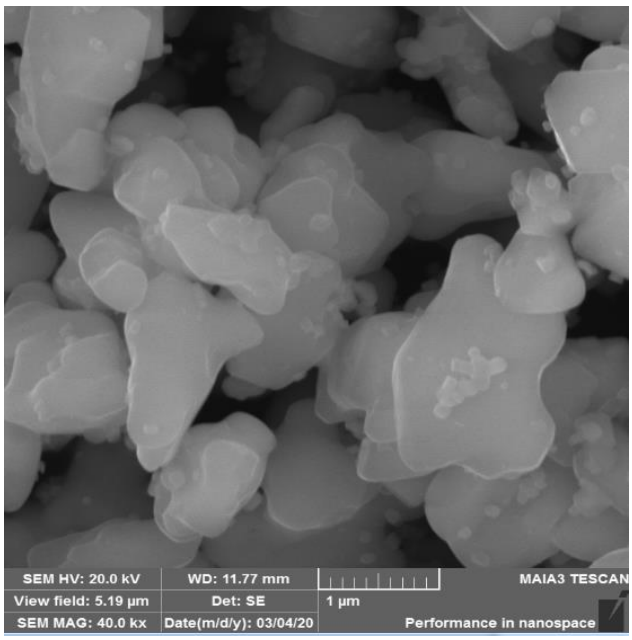

x = 0.2

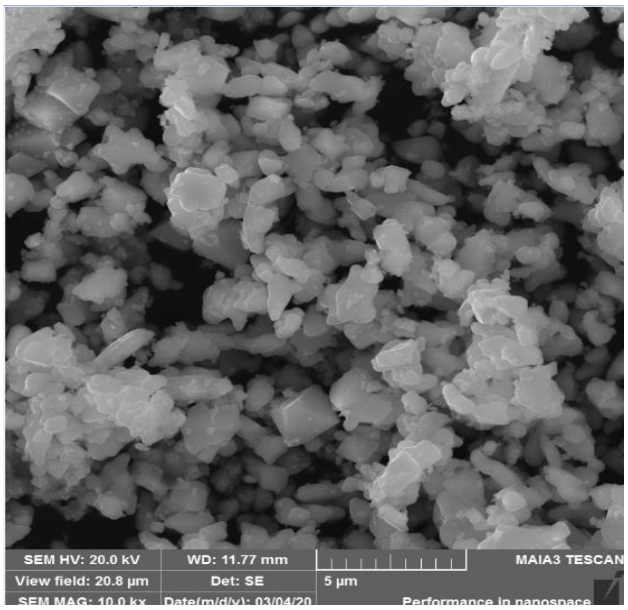

x = 0.4

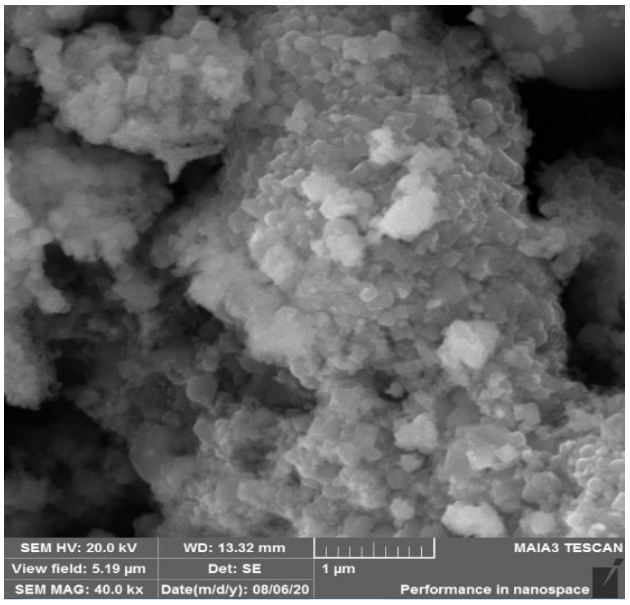

x = 0.6

Figure 3. SEM images of $Co_{1-x}Li_xCr_2O_4$ (x= 0.0, 0.2, 0.4 and 0.6).

3.3. Raman spectroscopy:

Raman spectroscopy of lithium doped in cobalt chromite, with the concentrations of lithium as 0.0, 0.2, 0.4 and 0.6, was performed. Raman spectroscopy graph is plotted between intensity in (a.u), and Raman shift in cm^{-1} ranging from 1000 to 1600 cm^{-1} with spacing of 100 cm^{-1}, and peaks are obtained at 1440 cm^{-1} and 1540 cm^{-1}, which shows the purity of sample. No impurity peak is observed in Raman Spectroscopy. Raman spectroscopy graph of lithium doped cobalt chromite is shown in Figure 4.

Preprints (www.preprints.org) | NOT PEER-REVIEWED | Posted: 6 May 2021 doi:10.20944/preprints202105.0085.v1

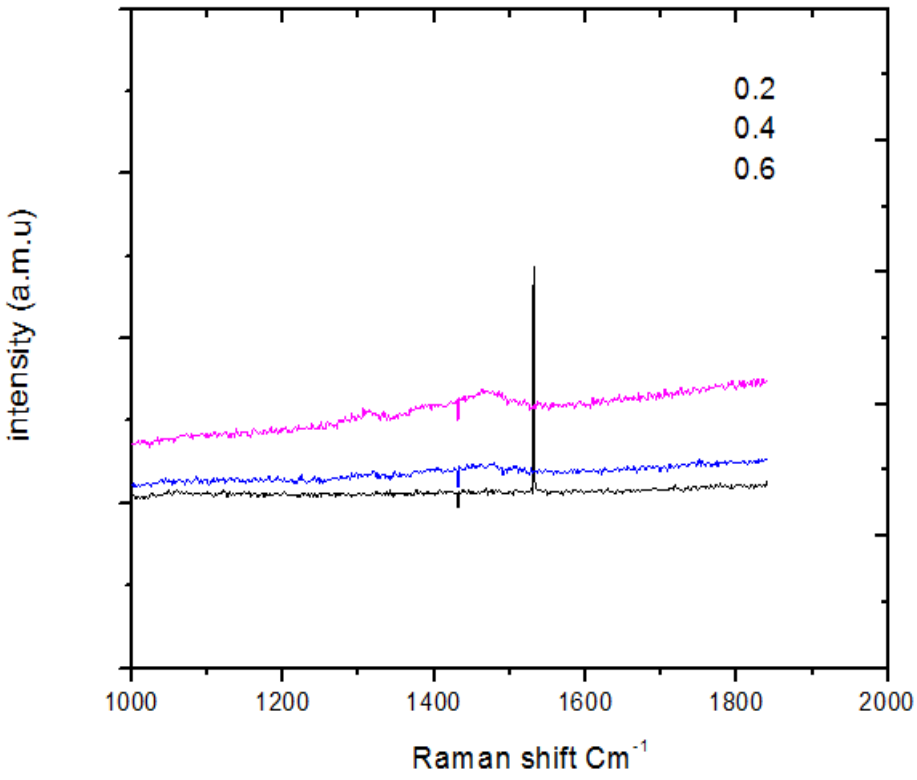

Figure 4. Raman spectroscopy of doped cobalt chromites $Co_{1-x}Ni_xCr_2O_4$.

3.4. Photoluminescence.

Figure 5 shows photoluminescence spectrum of nanoparticles. Excitation wavelength of 347 nm was used in this work at room temperature. It is important to monitoring that physical property of nanoparticles undergo changes with variation in their dimensions on nanometer scale, known as quantum size effect. For example, quantum confinement increases the required energy band gap of $CoCr_2O_4$ observed in Photoluminescence. The recombination of surface state is also evident from Photoluminescence. Photoluminence spectrum of Nanoparticle was performed at excitation wavelength 347nm at room temperature. The spectrum exhibit two emission peaks, one is located at 380 nm in the UV region, corresponding to near band gap excitonic emission. Second peak is positioned around 530 nm which can be attributed to the occupancy of independently ionized Co vacancies. Furthermore, narrow size distribution of nanoparticles in luminescence with full width and half maximum (FWHM) only few in nanometers, is reported by spectrum.

Preprints (www.preprints.org) | NOT PEER-REVIEWED | Posted: 6 May 2021 doi:10.20944/preprints202105.0085.v1

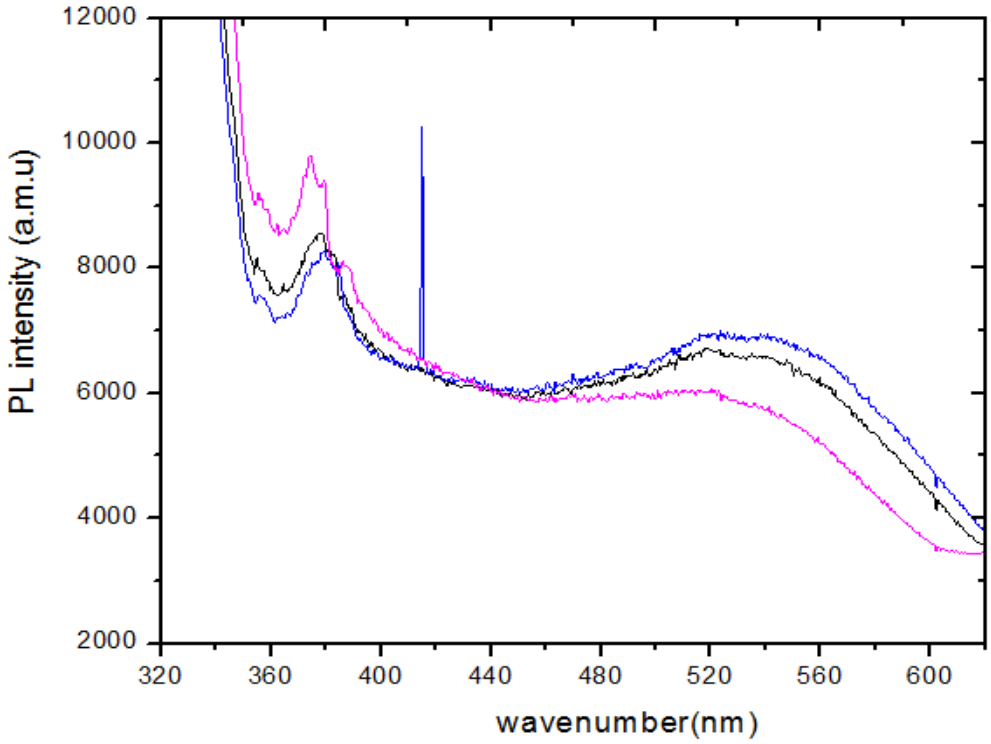

Figure 5. Photoluminescence spectra of doped $Co_{1-x}Li_xCr_2O_4$.

To put light on these compounds furthermore, the compounds prepared by the sol-gel synthesis route were formed with higher pronounced crystallinity. The morphological features of the samples derived by both synthesis methods are quite different. Moreover, the size and shape of chromite particles depend not only on the used synthesis method, but also on the nature of the octahedral cation A^{+2}. The origin of cation A^{+2} in the spinel structure displayed the tendency to produce pigments of numerous hues. The increase of Li^{+2}content leads to warm black color. The Co^{+2}enrichment in tetrahedral ligand field gives the variety of green shades form bluish green to yellowish green. Only Cu-doped pigments exhibited less different hues and are dark, nearly black. Nonetheless, there are no main differences of the colors between pigments, produced by the sol-gel synthesis methods. Due to these characteristic properties.

5. Conclusions

Chromites spinel $Co_{1-x}M_xCr_2O_4$ (M=Li with various concentration 0.2, 0.4 and 0.6) are synthesized by sol- gel method. Calcination temperature for single-phase cobalt chromites and Li-doped chromites were manufactured at 600-700˚C. Li substituted single-phase chromites were found to be dependent on annealing temperature. These spinels were mixture of spinel-type and spinel oxide at higher substitution ratios of 0.6. Outcomes revealed that cobalt chromites spinel structure was magnificently manufactured by conventional sol-gel method using chromium, Cobalt and copper nitrates as precursors under thermal decomposition. This method shows promising potential in the synthesis of $Co_{1-x}Li_xCr_2O_4$ for scale up production. Calcination temperature of 700˚C is necessary for obtaining spinel copper chromites. Results show that $Co_{1-x}Li_xCr_2O_4$ is very useful for engineered optical and electronic devices.

Conflict of Interests. All authors declare that this review article has neither been published, nor under consideration

for publication elsewhere. All authors have no conflicts of interest to declare.

Funding. The authors extend their sincere appreciation to the Deanship of Scientific Research at Princess Norah Bint Abdulrahman University, for the support through the Fast-track Research Funding Program.

Author Contribution. We acknowledge that all authors have contributed to this work and they all have seen and approved this work.

Acknowledgement. We acknowledge Princess Norah bint Abdulrahman University, Riphah International University and the University of Alabama at Birmingham for using their research labs, and computing facilities.

References

1. S. Mourdikoudis, R.M. Pallares, and N.T.K. Thanh. Characterization techniques for nanoparticles: comparison and complementarity upon studying nanoparticle properties. Nanoscale 10, 12871 – 12934 (2018)
2. Ib. Khan, K. Saeed, and Id. Khan, Nanoparticles: Properties, applications and toxicities. Arabian Journal of Chemistry 12(7), 908 – 931 (2019)
3. Anupreet Kaur and Usha Gupta, A review on applications of nanoparticles for the preconcentration of environmental pollutants. Journal of Materials Chemistry 19, 8279-8289 (2009).
4. Xiangjun Han, Ke Xu, Olena Taratula, Khashayar Farsad. Applications of nanoparticles in biomedical imaging. Nanoscale 11, 799-819 (2018).
5. M.S. Chavali and M.P. Nikolova. Metal oxide nanoparticles and their applications in nanotechnology. SN Applied Sciences 1, 607 (2019)
6. N. Castro-Alarcón, J.L. Herrera-Arizmendi, L.A. Marroquín-Carteño,I.P. Guzmán-Guzmán, A. Pérez-Centeno, M.A. Santana-Aranda. Antibacterial activity of nanoparticles of titanium dioxide, intrinsic and doped with indium and iron. Microbiol Res Int 4(4), 55–62 (2016).
7. M.R. Bindhu, M. Umadevi, M. K. Micheal, M.V. Arasu, N.A. Al-Dhabi. Structural, morphological, and optical properties of MgO nanoparticles for antibacterial applications. Mater. Let.t 166, 19–22 (2016).
8. D. Zakutna, I. Matulkova, E. Kentzinger, R. Medlin, Y. Su, K. Nemkovski, S. Disch, J. Vejpravova, and D. Niznansky. Dispersible cobalt chromite nanoparticles: facile synthesis and size driven collapse of magnetism. RSC Advances 6, 107659 – 107668 (2016).
9. P.L. Mahapatra, P.P. Mondal, S. Das, and D. Saha. Novel capacitive humidity sensing properties of cobalt chromite nanoparticles based thick film. Micheochemical Journal 152, 104452 (2020).
10. L.K.C. de Souza, J.R. Zamian, G.N. da Rocha Filho, et al. Blue pigments based on $Co_xZn_{1-x}Al_2O_4$ spinels synthesized by the polymeric precursor method. Dyes Pigments 81(3): 187-192 (2009).
11. G. Lorenzi, G. Baldi, F. Di Benedetto, V. Faso, P. Lattanzi, M. Romanelli, Spectroscopic study of a Ni-bearing gahnite pigment. J. . Ceram. Soc. 26: 317-321 (2006).
12. K.E. Sickafus, J.M. Wills, N.W. Grimes, Structure of spinel. J. Am. Ceram. Soc. 82: 3279-3292 (1999).
13. Z.W. Wang, P. Lazor, S.K. Saxena, G. Artioli, High-pressure Raman spectroscopic study of spinel (ZnCr2O4). J. Solid State Chem. 165: 165-170 (2002).
14. Z.W. Wang, P. Lazor, S.K. Saxena, G. Artioli, High-pressure Raman spectroscopic study of spinel (ZnCr2O4). J. Solid State Chem. 165: 165-170 (2002).
15. V.I. Torgashev, A.S. Prokhorov, G.A. Komandin, et al. Magnetic and dielectric response of cobalt-chromium spinel CoCr2O4 in the terahertz frequency range. Physics of the Solid State 54: 350-359 (2012).
16. G. Lawes, B. Melot, K. Page, C. Ederer, M.A. Hayward, Th. Proffen and R. Seshadri, Dielectric anomalies and spiral magnetic order in $CoCr_2O_4$. Phys. Rev. B 74: 024413 (2006).

17. V. Tsurkan, S. Zherlitsyn, S. Yasin, V. Felea, Y. Skourski, J. Deisenhofer, H.-A. Krug von Nidda, J. Wosnitza and A. Loidl. Unconventional Magnetostructural Transition in CoCr2O4 at High Magnetic Fields. Phys. Rev. Lett. 110: 115502 (2013).
18. Y. Yamasaki, S. Miyasaka, Y, Y. Kaneko, J.-P. He, T. Arima and Y. Tokura. Magnetic Reversal of the Ferroelectric Polarization in a Multiferroic Spinel Oxide. Phys. Rev. Lett. 96: 207204 (2006).
19. L. Kumar, P. Mohanty, T. Shripathi and C. Rath, Appearance of superparamagnetic phase below curie temperature in cobalt chromite. Nanoscience Nanotechnology Letters 1: 199-202 (2009).
20. D. Zakunta, J. Vlcek, P. Fitl, K. Nemokovski, D. Honecker, D. Niznansky and S. Disch. Noncollinear magnetism in nanosized cobalt chromite. Phys. Rev B 98: 064407 (2018).
21. M.R. Suchomel, D.P. Shoemaker, L. Ribaud, M.C. Kemei and R. Seshadri. Spin-induced symmetry breaking in orbitally ordered $NiCr_2O_4$ and $CuCr_2O_4$. Phys. Rev. B 86: 54406 (2012).
22. P. Mohanty, C.J. Sheppard, A.R.E. Prinsloo, W.D. Roos, L. Olivi and G. Aquilanti. Effect of cobalt substitution on the magnetic properties of nickel chromite. J. Magn. Magn. Mater. 451: 20-28 (2018).
23. P. Mohanty, A.R.E. Prinsloo, B.P. Doyle, E. Carleschi and C.J. Sheppard. Structural and magnetic properties of $(Co_{1-x}Ni_x)Cr_2O_4$ (x = 0.5, 0.25) nanoparticles. AIP Advances 8, 056424 (2018).
24. O. Opuchovic, G. Kreiza, J. Senvaitiene, K. Kazlauskas, A. Beganskiene, A. Kareiva. Sol-Gel synthesis, characterization and application of selected sub-microsized lanthanide (Ce, Pr,Nd, Tb) ferrites. Dyes Pigments 118, 176-182 (2015).
25. L. Kumar, P. Mohanty, T. Shripathi and C. Rath, Appearance of superparamagnetic phase below curie temperature in cobalt chromite. Nanoscience Nanotechnology Letters 1: 199-2002 (2009).